

Free vibration analysis of damaged beams via refined models

Marco Petrolo^{*1}, Erasmo Carrera^{1a} and Ali Saeghier Ali Saeed Alawami^{2b}

¹*Department of Mechanical and Aerospace Engineering, Politecnico di Torino,
Corso Duca degli Abruzzi 24, 10129 Torino, Italy*

²*School of Aerospace, Mechanical and Manufacturing Engineering, RMIT University,
Bundoora VIC 3083, Australia*

(Received April 30, 2015, Revised July 6, 2015, Accepted July 10, 2015)

Abstract. This paper presents the free vibration analysis of damaged beams by means of 1D (beam) advanced finite element models. The present 1D formulation stems from the Carrera Unified Formulation (CUF), and it leads to a Component-Wise (CW) modelling. By means of the CUF, any order 2D and 1D structural models can be developed in a unified and hierarchical manner, and they provide extremely accurate results with very low computational costs. The computational cost reduction in terms of total amount of DOFs ranges from 10 to 100 times less than shell and solid models, respectively. The CW provides a detailed physical description of the real structure since each component can be modelled with its material characteristics, that is, no homogenization techniques are required. Furthermore, although 1D models are exploited, the problem unknown variables can be placed on the physical surfaces of the real 3D model. No artificial surfaces or lines have to be defined to build the structural model. Global and local damages are introduced by decreasing the stiffness properties of the material in the damaged regions. The results show that the proposed 1D models can deal with damaged structures as accurately as a shell or a solid model, but with far lower computational costs. Furthermore, it is shown how the presence of damages can lead to shell-like modal shapes and torsional/bending coupling.

Keywords: Carrera unified formulation; beam; finite element; advanced models; damage analysis

1. Introduction

Computational models for the analysis of damaged structures should be able to provide very accurate displacement, strain and stress fields. Damages may lead, in fact, to local and non-classical effects that require 3D-like analysis capabilities. Currently, most of the techniques that have been developed for these tasks are based on very cumbersome numerical models, such as the 3D solid finite elements. The accurate structural analysis of complex structures is almost impossible due to the enormous number of degrees of freedom that is required.

Beam models are widely adopted for many structural engineering applications because they are computationally cheaper and less cumbersome than a plate, shell or solid finite element model.

*Corresponding author, Postdoctoral Research Fellow, E-mail: marco.petrolo@polito.it

^aProfessor, E-mail: erasmo.carrera@polito.it

^bUndergraduate Student, E-mail: s3140385@student.rmit.edu.au

The classical beam theories are those by Euler-Bernoulli (Euler 1744 and Bernoulli 1751) and Timoshenko (1921). None of these theories can detect non-classical effects such as warping, out-and in-plane deformations, torsion-bending coupling or localized boundary conditions (geometrical or mechanical). These effects are important when, for instance, small slenderness ratios, thin walls, the anisotropy of the materials and damages are considered.

Many methods have been proposed over the last decades to enhance classical theories and to extend the application of 1D models to any geometry or boundary condition. Recent developments in 1D models have been obtained by means of various approaches. Such as,

- The introduction of shear correction factors (Timoshenko 1921).
- The use of warping functions based on the Saint-Venant solution (Ladéveze *et al.* 2004, El Fatmi and Ghazouani 2011).
- Asymptotic approaches (Berdichevsky 1992).
- Generalized beam theories (GBT) (Schardt 1994).
- Higher-order beam models (Kapania and Raciti 1989a,b).

This work exploits the Carrera Unified Formulation (CUF) for higher-order 1D models (Carrera 2002, Carrera *et al.* 2011, 2014). CUF was initially developed for plates and shells (Carrera 2002, 2003), more recently for beams (Carrera and Giunta 2010, Carrera *et al.* 2010a, 2011). In CUF models, the displacement field above the cross-section is modelled through expansion functions whose order is a free parameter of the analysis. In other words, any order structural models can be implemented with no need for formal changes in the problem equations and matrices. CUF can, therefore, deal with arbitrary geometries, boundary conditions and material characteristics with no need of ad hoc formulations.

CUF 1D models have recently been applied to static (Carrera and Giunta 2010, Carrera *et al.* 2010a, 2012c) and free vibration (Carrera *et al.* 2010b) analyses. The most recent extension of CUF models is the so-called Component-Wise approach (CW). The CW is based on the use of Lagrange polynomials for the cross-section displacement field description (Carrera and Petrolo 2012a,b). Multicomponent structures (e.g., aircraft wings or fibre reinforced composites) are modelled through a unique 1D formulation (Carrera *et al.* 2012a,b, 2013a,b). 1D CW leads to solid-like accuracies with far less computational costs than the shell and solid FEs.

In this work, CUF 1D models are exploited to analyse damaged structures through the free vibration analysis. The numerical and experimental analysis of damaged structures is usually carried out for damaged identification purposes. In particular, the damage detection has various tasks. Such as the detection of presence of damage, the quantification of the damage, the detection of the position of the damage, and the estimation of the remaining service life of the structure (Fayyadh *et al.* 2011). As well-known, the presence of damages affects the natural frequencies of a structure, and this has been exploited to develop damage detection techniques in many works. Some of the most recent papers on this topic are presented hereinafter. Zhang *et al.* (2014) have proposed a graphical technique to detect the location and severity of delamination in composite beams by studying the frequency shifts induced by such damages. Capozucca (2014) has studied the vibration response of damaged Carbon Fibre Reinforced Polymer (CFRP) beams. Pérez *et al.* (2014) have conducted an extensive experimental activity to investigate the effects of damages on the vibrations of composite laminates. Wang *et al.* (2014) have proposed a method for the damage detection and diagnosis in wind turbine blades that is based on the FEM dynamic analysis and the variation of the modal shape curvatures.

A number of damage detection techniques have been recently proposed that exploit the Modal Assurance Criterion or its variations. The MAC is defined as a scalar representing the degree of

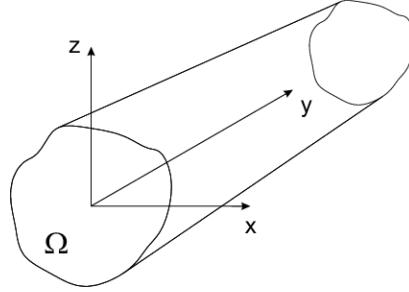


Fig. 1 Coordinate frame of the beam model

consistency (linearity) between one modal and another reference modal vector (Allemang and Brown 1982). Salawu and Williams (1995) exploited the MAC and Coordinate Modal Assurance Criterion (COMAC) for the damage analysis of bridges. More recent papers on the same topic are those by Zhao and Zhang (2012), Mukhopadhyay *et al.* (2012), Balsamo *et al.* (2013). A comprehensive and detailed description of the main computational tools for damage detection can be found in the book of Gopalakrishnan *et al.* (2011).

This paper investigates frequency shifts, modal shape changes and MAC variations due to damages in isotropic beams. The aim of this paper is to highlight the advanced capabilities of refined 1D models for the analysis of globally and locally damaged structures, and its potential applications to damage detection techniques.

This paper is organized as follows: Section 2 provides a brief theoretical overview on the structural model adopted, numerical results are given and discussed in Section 3, and conclusions are drawn in Section 4.

2. Carrera unified formulation and damage modelling

The cross-section of the beam lies on the xz -plane, and it is denoted by Ω , whereas the boundaries over y are $0 \leq y \leq L$. Fig. 1 shows the adopted rectangular Cartesian coordinate system. The transposed displacement vector is

$$\mathbf{u}(x, y, z; t) = \{u_x \ u_y \ u_z\}^T \quad (1)$$

Within the framework of the CUF, the 3D displacement field of Eq. (1) is expressed as

$$\mathbf{u}(x, y, z; t) = F_\tau(x, z)\mathbf{u}_\tau(y; t), \quad \tau = 1, 2, \dots, M \quad (2)$$

Where F_τ are the functions of the coordinates x and z on the cross-section. \mathbf{u}_τ is the vector of the generalized displacements. M stands for the number of the terms used in the expansion, and the repeated subscript, τ indicates summation. TE (Taylor Expansion) 1D CUF models consist of McLaurin series that uses the 2D polynomials $x^i z^j$ as F_τ functions, where i and j are positive integers. For instance, the displacement field of the second-order ($N = 2$) TE model can be expressed as

$$u_x = u_{x_1} + x u_{x_2} + z u_{x_3} + x^2 u_{x_4} + xz u_{x_5} + z^2 u_{x_6}$$

$$\begin{aligned} u_y &= u_{y_1} + x u_{y_2} + z u_{y_3} + x^2 u_{y_4} + xz u_{y_5} + z^2 u_{y_6} \\ u_z &= u_{z_1} + x u_{z_2} + z u_{z_3} + x^2 u_{z_4} + xz u_{z_5} + z^2 u_{z_6} \end{aligned} \quad (3)$$

The $N = 2$ model has 18 generalized displacement variables. The order N of the expansion is set as an input to the analysis; the integer N is arbitrary, and it defines the order of the beam theory. Classical Euler-Bernoulli (EBBT) and Timoshenko (TBT) beam theories can be realized as degenerated cases of the linear ($N = 1$) TE model. For further information about TE models see (Carrera *et al.* 2011).

LE (Lagrange Expansion) 1D CUF models exploit 2D Lagrange polynomials to model the displacement field of the structure above the cross-section. For instance, the displacement field of an L9 LE model can be expressed as

$$\begin{aligned} u_x &= L_1 u_{x_1} + L_2 u_{x_2} + L_3 u_{x_3} + L_4 u_{x_4} + L_5 u_{x_5} + L_6 u_{x_6} + L_7 u_{x_7} + L_8 u_{x_8} + L_9 u_{x_9} \\ u_y &= L_1 u_{y_1} + L_2 u_{y_2} + L_3 u_{y_3} + L_4 u_{y_4} + L_5 u_{y_5} + L_6 u_{y_6} + L_7 u_{y_7} + L_8 u_{y_8} + L_9 u_{y_9} \\ u_z &= L_1 u_{z_1} + L_2 u_{z_2} + L_3 u_{z_3} + L_4 u_{z_4} + L_5 u_{z_5} + L_6 u_{z_6} + L_7 u_{z_7} + L_8 u_{z_8} + L_9 u_{z_9} \end{aligned} \quad (4)$$

The L9 model has 27 displacement variables that coincide with the three displacement components of the 9 Lagrange nodes. Fig. 2 shows an example of L9 element. Two or more Lagrange elements can be conveniently assembled to discretized cross-sections, and improve the accuracy of the model. More details about LE models can be found in (Carrera *et al.* 2014).

The governing equations were derived by means of the Principle of Virtual Displacements (PVD). A compact form of the virtual variation of the strain energy can be obtained as shown in (Carrera *et al.* 2014),

$$\delta L_{int} = \delta \mathbf{q}_s^T \mathbf{K}^{ij\tau s} \mathbf{q}_{\tau i} \quad (5)$$

Where $\mathbf{K}^{ij\tau s}$ is the stiffness matrix written in the form of the fundamental nuclei whose components can be found in (Carrera *et al.* 2014). δ indicates the virtual variation. Superscripts indicate the four indexes exploited to assemble the matrix: i and j are related to the shape functions, τ and s are related to the expansion functions. The fundamental nucleus is a 3×3 array that is formally independent of the order of the beam model. It should be underlined that the formal expression of $\mathbf{K}^{ij\tau s}$

1. Does not depend on the expansion order.
2. Does not depend on the choice of the F_τ expansion polynomials.

These are the key-points of CUF, which permits, with only nine FORTRAN statements, to implement any order of multiple class theories.

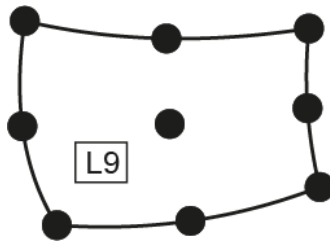


Fig. 2 L9 cross-section element

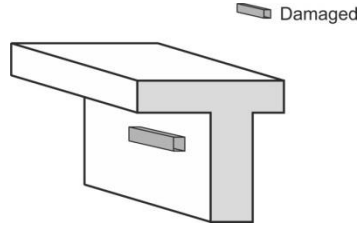


Fig. 3 A locally damaged structure

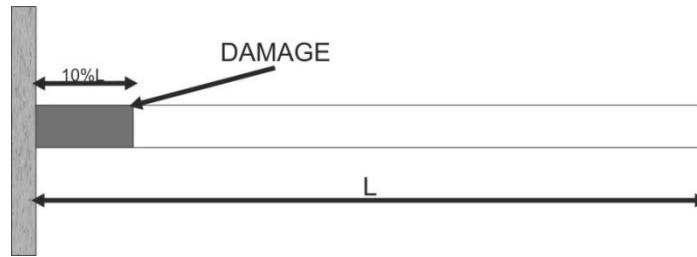


Fig. 4 Damage at the root of a cantilever

The virtual variation of the work of the inertial loadings is

$$\delta L_{ine} = \int_V \rho \dot{\mathbf{u}} \delta \mathbf{u}^T dV \quad (6)$$

Where ρ stands for the density of the material, and $\dot{\mathbf{u}}$ is the acceleration vector. Eq. (6) can be rewritten in a compact manner as follows

$$\delta L_{ine} = \delta \mathbf{q}_{sj}^T \mathbf{M}^{ij\tau s} \ddot{\mathbf{q}}_{\tau i} \quad (6)$$

Where $\mathbf{M}^{ij\tau s}$ is the mass matrix in the form of the fundamental nucleus whose components can be found in (Carrera *et al.* 2014).

A basic damage modelling approach was adopted in this work. Fig. 3 shows an example of locally damaged structure. In the damaged zone, the material characteristics were modified according to the following formulas

$$E_d = d \times E \text{ with } 0 \leq d \leq 1 \quad (7)$$

Damages were introduced in different portions of the structure as will be shown in the result section of this paper.

3. Results and discussion

Numerical assessments were carried out on a square beam and a thin-walled I-beam. Different damage spatial distributions were considered. Fig. 4 shows a typical longitudinal distribution of the damage in which the first 10% of the beam was affected. Hereinafter, such a configuration is referred to as “damaged root”. Other two distributions were considered; the “damaged free end” has the last 10% of the beam damaged, whereas the “damaged center” has the central 10% of the

Table 1 Effect of the CUF 1D expansion order (N) on the first three vibration frequencies (Hz) of the undamaged and damaged square beam, $d=0.1$

	Model	EBBT	TBT	$N=1$	$N=2$	$N=3$	$N=4$	Solid
	DOFs	183	305	549	1098	1647	2196	139587
Undamaged	1 st	42.5 ^b	42.3 ^b	42.3 ^b	42.6 ^b	42.6 ^b	42.5 ^b	42.4 ^b
	2 nd	263.2 ^b	254.5 ^b	254.5 ^b	256.2 ^b	256.2 ^b	254.7 ^b	254.0 ^b
	3 rd	658.8 ^a	658.8 ^a	403.9 ^t	403.9 ^t	403.9 ^t	372.1 ^t	369.7 ^t
Damaged Free End	1 st	42.5 ^b	42.3 ^b	42.3 ^b	42.6 ^b	42.5 ^b	42.5 ^b	42.4 ^b
	2 nd	262.2 ^b	252.6 ^b	252.6 ^b	254.3 ^b	252.8 ^b	252.7 ^b	252.0 ^b
	3 rd	653.6 ^a	642.1 ^a	400.8 ^t	400.8 ^t	400.8 ^t	369.2 ^t	366.9 ^t
Damaged Center	1 st	35.4 ^b	35.2 ^b	35.2 ^b	35.7 ^b	35.6 ^b	35.6 ^b	35.4 ^b
	2 nd	174.5 ^b	170.6 ^b	170.6 ^b	173.8 ^b	173.0 ^b	172.8 ^b	172.1 ^b
	3 rd	467.0 ^a	467.0 ^a	286.3 ^t	286.3 ^t	286.3 ^t	265.8 ^t	263.4 ^t
Damaged Root	1 st	20.8 ^b	20.7 ^b	20.7 ^b	21.3 ^b	21.3 ^b	21.2 ^b	21.1 ^b
	2 nd	210.8 ^b	198.1 ^b	198.1 ^b	199.2 ^b	197.5 ^b	197.4 ^b	196.8 ^b
	3 rd	381.5 ^a	381.5 ^a	233.9 ^t	233.9 ^t	233.9 ^t	218.3 ^t	216.0 ^t

b: Bending mode; a: Axial mode; t: Torsional mode

Table 2 Effect of the damage level and location on the on the first three vibration frequencies (Hz) of the square beam

	1 st Mode		2 nd Mode		3 rd Mode		
	Model	$N = 4$	Solid	$N = 4$	Solid	$N = 4$	Solid
	DOFs	2196	139587	2196	139587	2196	139587
Undamaged		42.5 ^b	42.4 ^b	254.7 ^b	254.0 ^b	372.1 ^t	369.7 ^t
Damaged Free End	$d = 0.7$	42.5 ^b	42.4 ^b	254.6 ^b	253.9 ^b	372.0 ^t	369.6 ^t
	$d = 0.4$	42.5 ^b	42.4 ^b	254.4 ^b	253.6 ^b	371.6 ^t	369.3 ^t
	$d = 0.1$	42.5 ^b	42.4 ^b	252.7 ^b	252.0 ^b	369.2 ^t	366.9 ^t
Damaged Center	$d = 0.7$	42.1 ^b	41.9 ^b	245.3 ^b	244.6 ^b	364.3 ^t	362.0 ^t
	$d = 0.4$	41.1 ^b	40.9 ^b	227.0 ^b	226.2 ^b	346.6 ^t	344.3 ^t
	$d = 0.1$	35.6 ^b	35.4 ^b	172.8 ^b	172.1 ^b	265.8 ^t	263.4 ^t
Damaged Root	$d = 0.7$	39.7 ^b	39.6 ^b	244.2 ^b	243.5 ^b	357.4 ^t	355.0 ^t
	$d = 0.4$	34.7 ^b	34.5 ^b	228.5 ^b	227.8 ^b	326.3 ^t	323.8 ^t
	$d = 0.1$	21.2 ^b	21.1 ^b	197.4 ^b	196.8 ^b	218.3 ^t	216.0 ^t

b: Bending mode; t: Torsional mode

beam damaged. Furthermore, in a few cases, the damage was introduced along the entire span of the beam. Various damage distributions above the cross-section were considered; they are described in the next sections.

3.1 Square cross-section beam

A cantilever beam was considered as first study case. The beam length (L), width (a), and

height (h) are equal to 2 m, 0.2 m, and 0.2 m, respectively. The material is isotropic; $E = 75$ GPa, $\nu = 0.33$, and $\rho = 2700$ Kg/m³.

Table 1 shows the first three natural frequencies of the beam via different beam models against a Solid element model in Abaqus. The number of degrees of freedom (DOFs) of each model is given in the second row of the table. The entire cross-section was damaged. A severe damage level was considered ($d = 0.1$); such a choice was made to carry out a convergence study on the beam models and find the most appropriate expansion order to meet the Solid model accuracy. As it can be seen from Table 1, the $N = 4$ beam model offers satisfactory accuracies both for bending and torsional modes. The $N = 4$ model was then used for all the subsequent analyses.

Table 2 shows the first three natural frequencies of the beam for various damage levels and locations. Figs. 5-7 show the influence of the damage level on the frequency; in particular the ratio between the frequency of the damaged model (f_d) and the undamaged one (f) is depicted. Fig. 8 shows the effect of damage in a given location on the first three modal shapes.

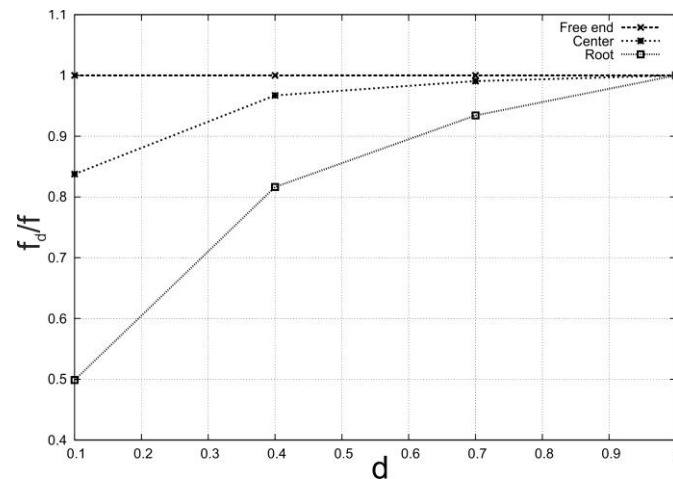


Fig. 5 Effect of the damage level and location on the first bending mode of the square beam, $N=4$

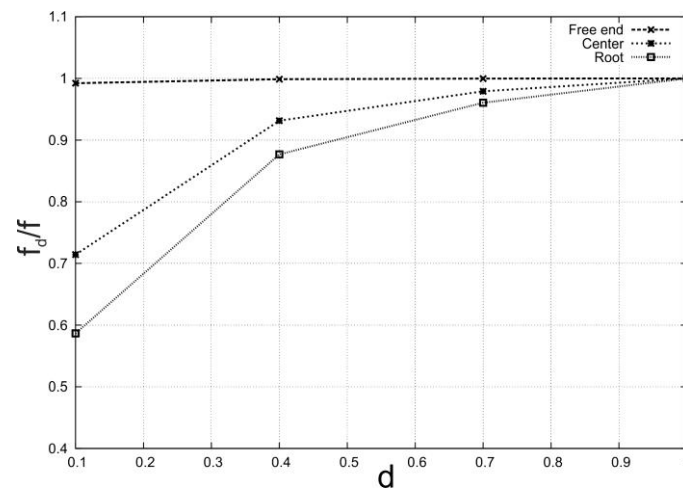


Fig. 6 Effect of the damage level and location on the first torsional mode of the square beam, $N=4$

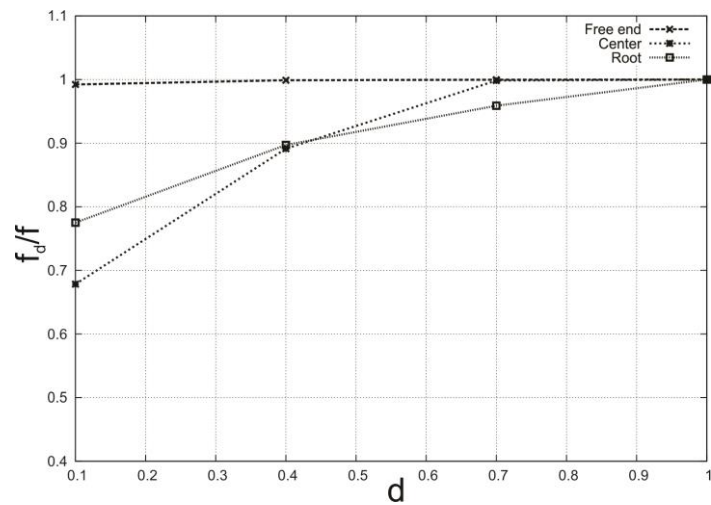


Fig. 7 Effect of the damage level and location on the second bending mode of the square beam, $N=4$

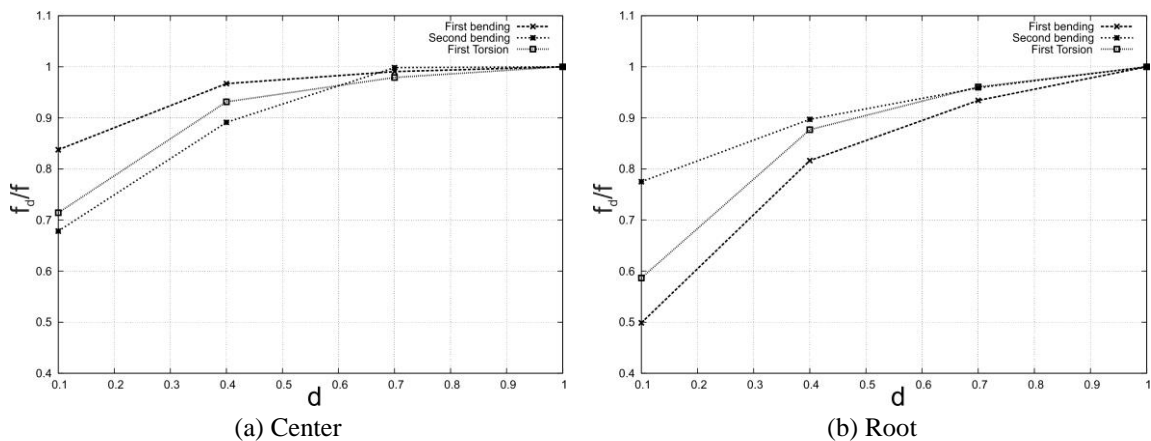


Fig. 8 Effect of the damage level and modal shape on the frequencies, $N=4$

The analysis of the deep square beam highlighted the following main points:

- A fourth-order beam model ($N = 4$) is needed to deal with damaged beams as accurately as via a solid model. In particular, such a model is required to detect the torsional frequency of the beam. From past works of the authors, it is known that torsional frequencies require at least an $N = 2$ model. The presence of the damage worsens this requirement. Whereas bending modes can be detected properly by lower-order models. However, since a moderately thick beam was considered, at least the TBT is needed for the bending modes.
- As expected, the computational cost of the advanced beam models is very low with respect to the solid model.
- The effect of the damage on the natural frequencies, bending and torsional, is very low as soon as the damage is located at the free end.
- Damages of the central portion of the beam influence the natural frequencies more significantly than the free tip damage. In particular, as $d < 0.7$, the effects on the frequencies are

higher than 5%.

- Root damages affect the frequencies to a great extent even for low damage levels.
- The first bending mode should be used to detect root damages. The second bending mode is more affected by the central damages, whereas the effect of damage on the torsional frequency is generally in between those on the bending modes independently of the damage location, unless low damage levels are considered.
- For $1 < d < 0.7$, that is, up to 30% of stiffness reductions, the effect on the natural frequencies is lower than 10 %. For $0.7 < d < 0.4$, the effect on the natural frequencies is lower than 20 %. For $d < 0.5$, the effect on natural frequencies ranges from 20% to 50%.

6.2 Thin-walled, I-section beam

A cantilever thin-walled beam was considered as the second study case, as shown in Fig. 9; $L = 1$ m, $h = 0.1$ m, $b = 0.1$ m, and $t = 0.002$ m. The material is isotropic; $E = 75$ GPa, $\nu = 0.33$, and $\rho = 2700$ Kg/m³. Various damage distributions along the cross-section were employed, as shown in Fig. 10.

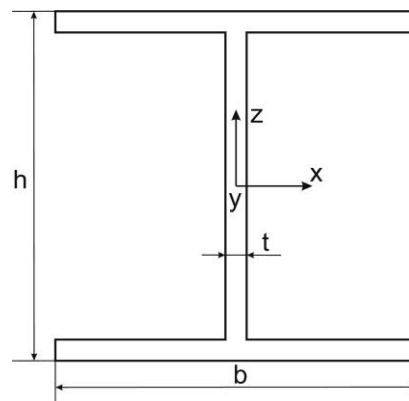


Fig. 9 I-Section

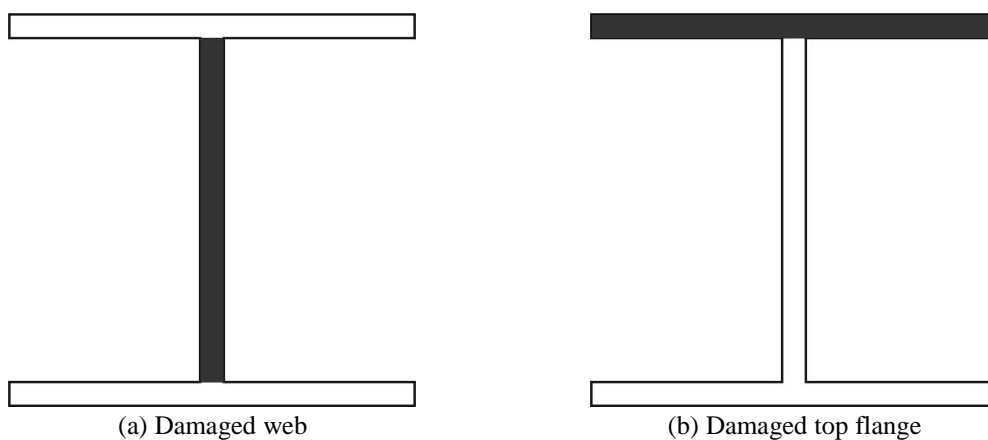
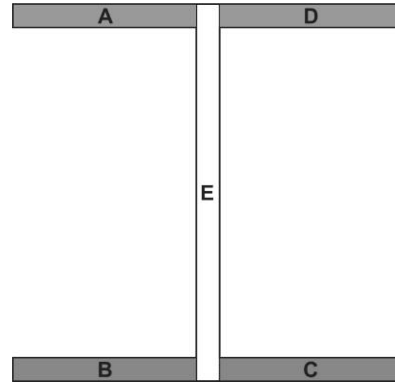


Fig. 10 Damage distribution along the I-section



(c) Multi-damage cross-section

Fig. 10 Continued

Table 3 Effect of the CUF 1D expansion order (N) on the first three vibration frequencies (Hz) of the undamaged and damaged I beam, damaged web

	Model	EBBT	TBT	N = 2	N = 4	N = 6	8L9	12L9	Shell
	DOFs	183	305	1098	2745	5124	4743	5625	27972
$d = 1$	1 st	69.9 ^b	69.7 ^b	70.3 ^b	69.9 ^b	69.7 ^b	69.7 ^b	69.8 ^b	69.2 ^b
	2 nd	127.0 ^b	125.6 ^b	126.3 ^b	123.9 ^b	116.4 ^t	73.8 ^t	73.8 ^t	72.8 ^t
	3 rd	434.7 ^b	424.7 ^b	428.6 ^b	152.0 ^t	123.3 ^b	122.7 ^b	122.6 ^b	119.8 ^b
	4 th	776.3 ^b	723.9 ^b	692.3 ^t	424.8 ^b	328.9 ^s	239.1 ^s	236.9 ^s	232.3 ^s
	5 th	1202.2 ^b	1142.0 ^a	727.4 ^b	550.0 ^t	411.0 ^b	252.8 ^s	251.1 ^s	246.3 ^s
$d = 0.1$	1 st	69.9 ^b	69.6 ^b	70.2 ^b	69.7 ^b	69.1 ^b	67.3 ^b	67.3 ^b	66.4 ^b
	2 nd	119.2 ^b	117.5 ^b	118.2 ^b	95.3 ^t	94.6 ^t	71.4 ^t	71.5 ^t	70.1 ^t
	3 rd	434.6 ^b	420.8 ^b	424.6 ^b	97.5 ^b	96.6 ^b	87.0 ^s	87.0 ^s	85.2 ^s
	4 th	728.3 ^b	668.6 ^b	671.2 ^b	361.7 ^b	142.7 ^s	93.9 ^b	93.8 ^b	91.7 ^b
	5 th	1108.8 ^a	1108.8 ^a	679.8 ^t	418.9 ^b	302.7 ^s	121.2 ^s	121.1 ^s	118.6 ^s

b: Bending mode; a: Axial mode; t: Torsional mode; s: Shell-like mode

Table 3 shows the first five frequencies of the I-beam in which the web was damaged along the entire span of the beam. Classical, TE, and LE beam models were considered and compared to a shell model built in Abaqus. The number of DOFs of each model is given in the second row. As in the previous case, the aim of this first assessment was a convergence analysis of the beam model to detect the shell solution. In this case, an LE model with 8 L9 elements was needed to obtain the shell solution for bending, torsional and shell-like modes. The latter indicates a mode that is usually detectable by shell elements. Fig. 11 shows a typical shell-like model in which the horizontal flanges of the beam undergo severe cross-sectional deformations. The 8 L9 model was then used for all the other I-beam analyses.

The top flange damaged configuration was then considered along the entire span. Fig. 12 shows the first five frequencies via the TBT, an 8 L9 beam, and a shell model. Fig. 13 shows the first five modal shapes that were obtained by means of the 8 L9 model.

The correspondence between the undamaged and damaged structure modal shapes is

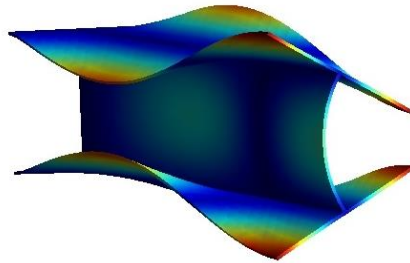
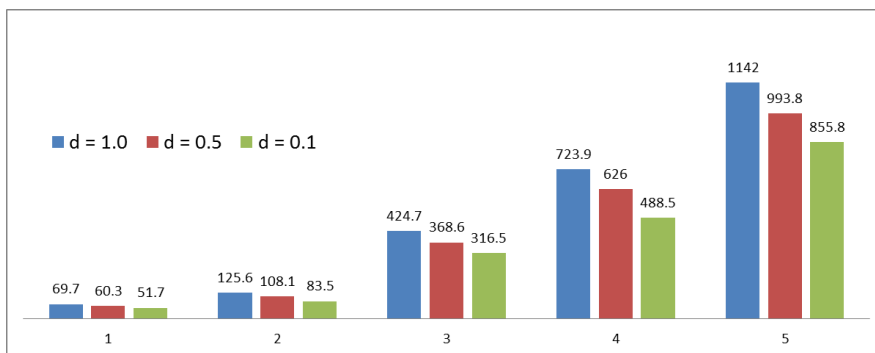
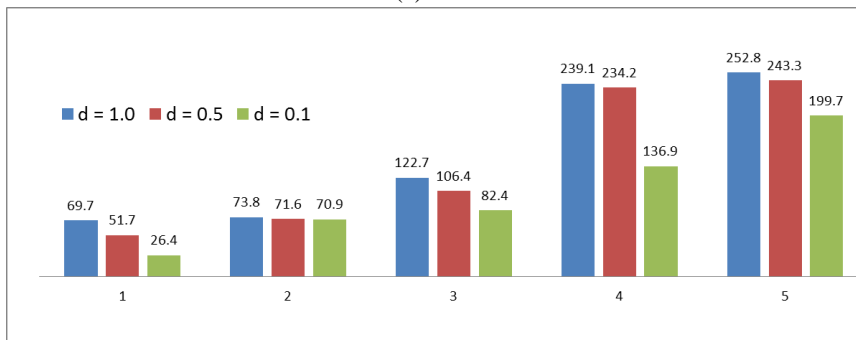


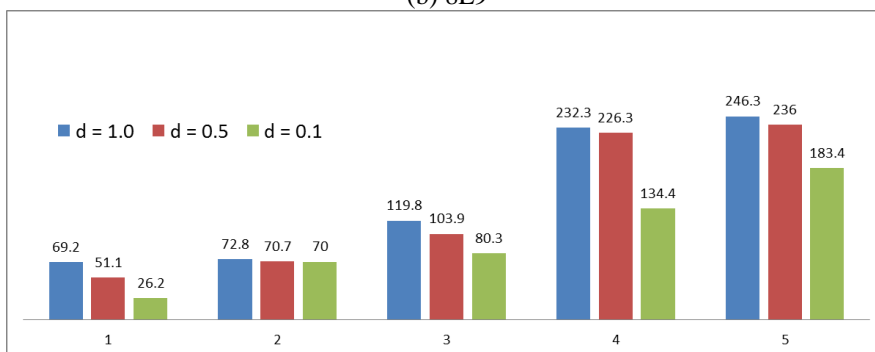
Fig. 11 I-Section shell-like mode, 8L9, $f = 252.8$ Hz



(a) TBT



(b) 8L9



(c) Shell

Fig. 12 Effect of the top flange damage level on the first five natural frequencies (Hz) of the I-beam via different models

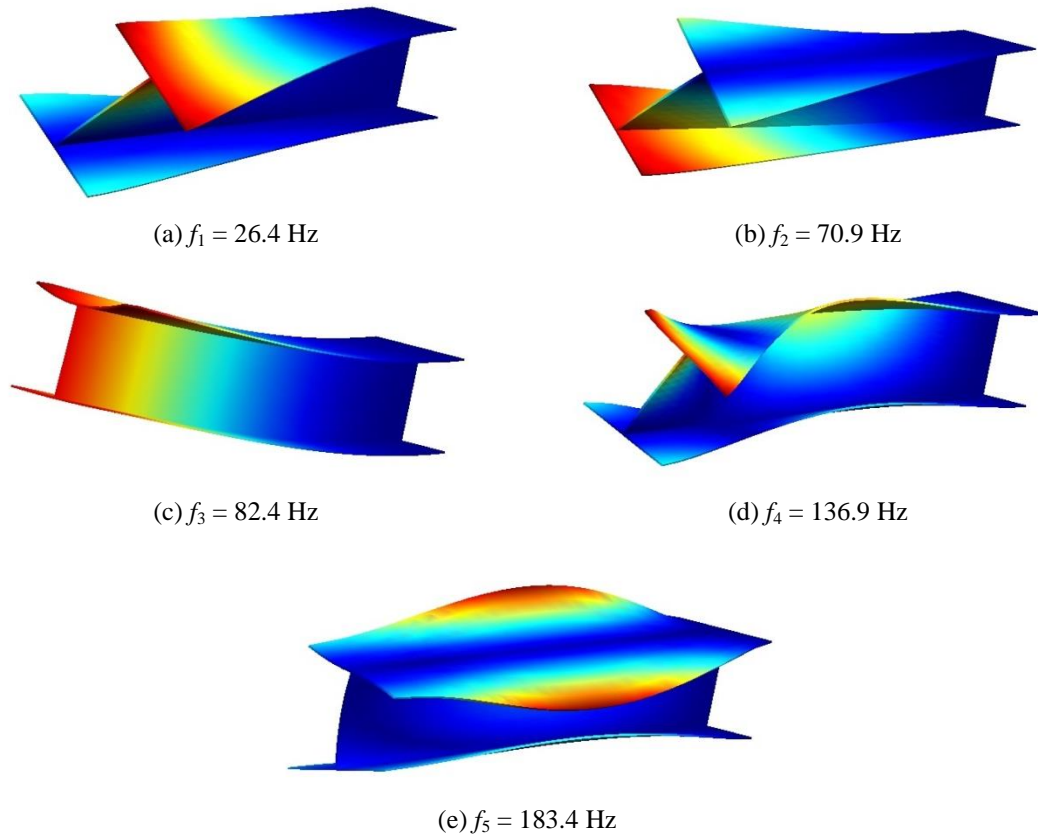


Fig. 13 First five natural modes of the I-Beam with the top flange damaged, 8 L9, $d = 0.1$

investigated through the Modal Assurance Criterion (MAC).

Fig. 14 shows the MAC matrices in which the damaged and undamaged beams are compared; the entire span damaged top flange and web were considered.

The analyses of the top and web damaged beams has highlighted suggest that

- Thin-walled beams require LE models to deal with torsion and shell-like modes in which severe cross-sectional deformations may occur. Such models are as accurate as shell FEs, but fewer DOFs are required.
- The presence of damage makes the use of LE necessary even for bending modes. LE are, in fact, component-wise models in which the local material and geometrical characteristics are retained, and LE can be locally refined where needed. All these features make the detection of local effects, due, for instance, to local stiffness losses, easier to deal with.
- As known from previous works of the authors, classical beam models provide acceptable accuracies for bending modes only. However, since damage can cause bending-torsion coupling, the use of classical beam models for damaged structures should be avoided.
- The effect of a damage on a natural frequency depends on the modal shape to a great extent. In other words, as soon as a damage is in place, there may be a shift in the modal shapes with respect to the undamaged configuration. For instance, shell-like modes could appear with lower

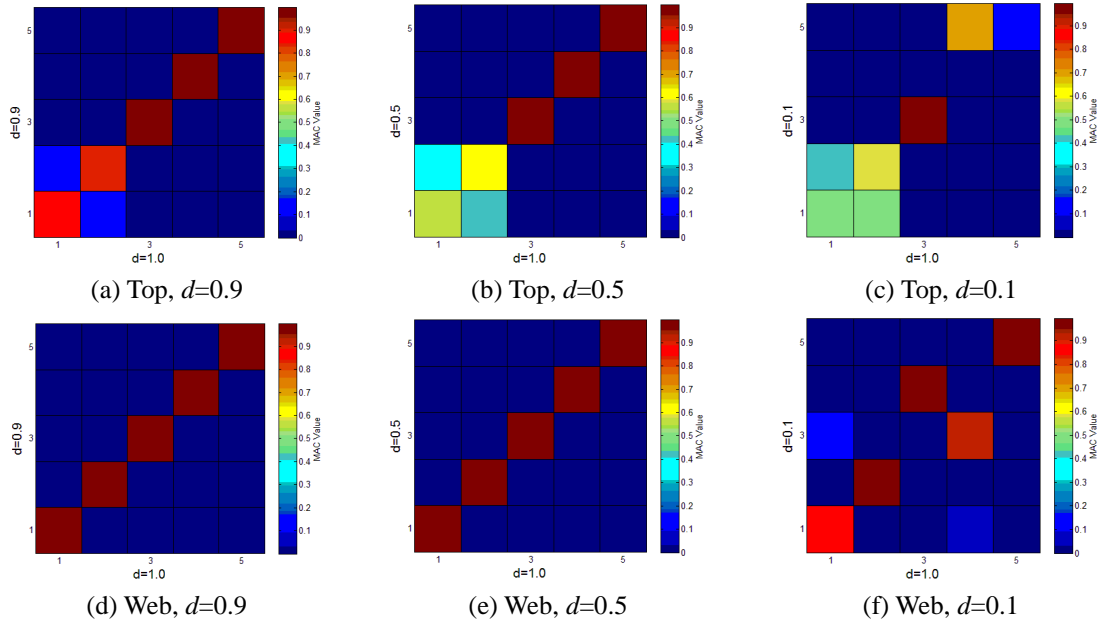


Fig. 14 MAC matrices for the I-Beam, damaged vs. undamaged configurations, 8L9

Table 4 Damage distribution sets of the multi-damage cross-section

	A	B	C	D	E
Set 1, $d =$	0.5	0.7	0.8	0.6	0.9
Set 2, $d =$	0.1	0.7	0.1	0.6	0.9

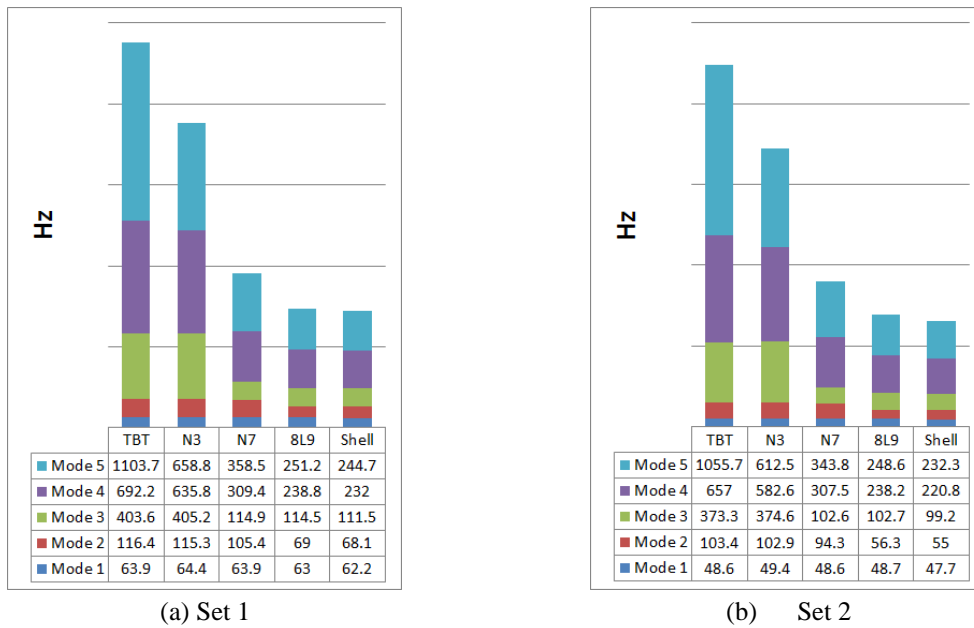


Fig. 15 First five natural frequencies of the multi-damage cross-section beam

frequencies than bending modes. Higher the damage, more important this effect.

- LE models can deal with the latter effect as accurately as shell models.
- The effect of the damage on the MAC matrix is hardly detectable for $d < 0.9$ even if the damage is present in large portions of the beam.

Inhomogeneous damage distributions above the cross-section were then considered (see Fig. 10(c)). Table 4 shows the damage distribution above the cross-section; damages were introduced along the first 10% of the beam (root damage).

Fig. 15 shows the first five frequencies that were computed by TBT, TE, LE, and shell models. Figs. 16 and 17 show the first five modes that were obtained via the LE model. Fig. 18 shows the MAC matrix in which the damaged beam modes are compared with the undamaged ones; in both cases, the LE model was employed.

The analysis of the multi-damage beam suggests that

- A perfect match was found between the LE and shell solutions. The first five modes of both

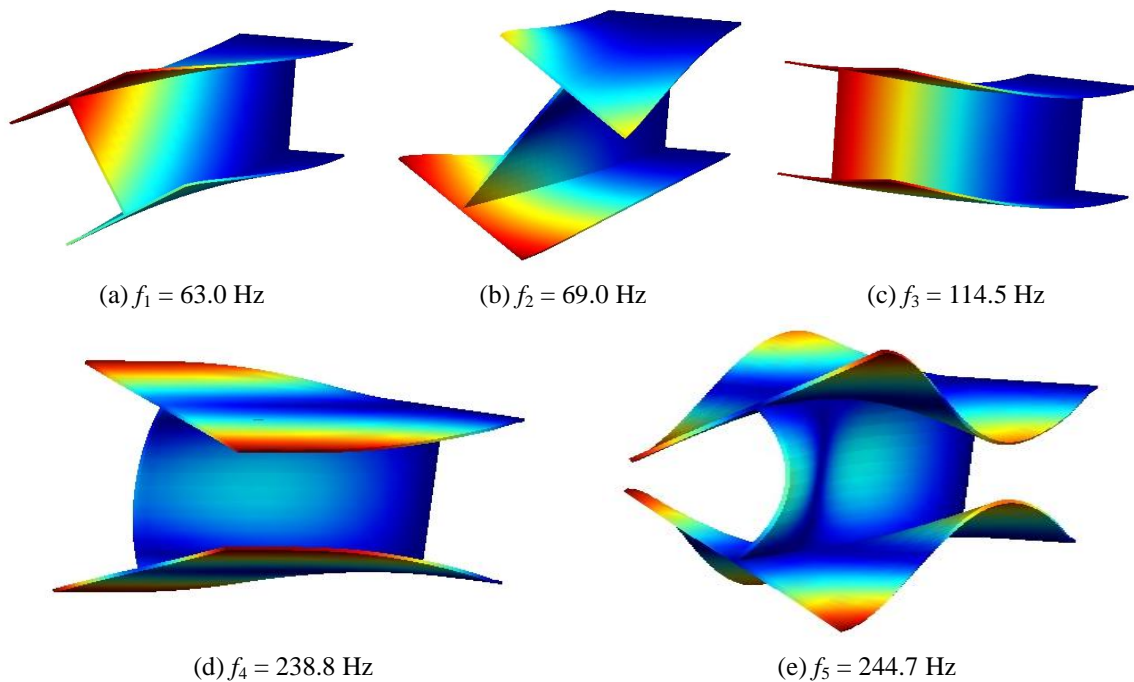


Fig. 16 First five modal shapes of the multi-damage cross-section beam, Set 1, 8L9

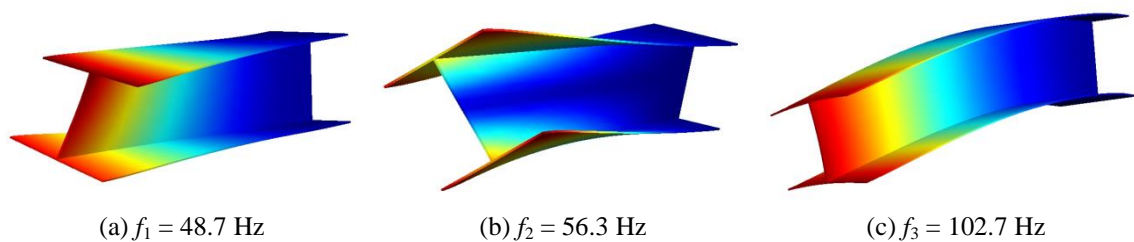


Fig. 17 First five modal shapes of the multi-damage cross-section beam, Set 2, 8L9

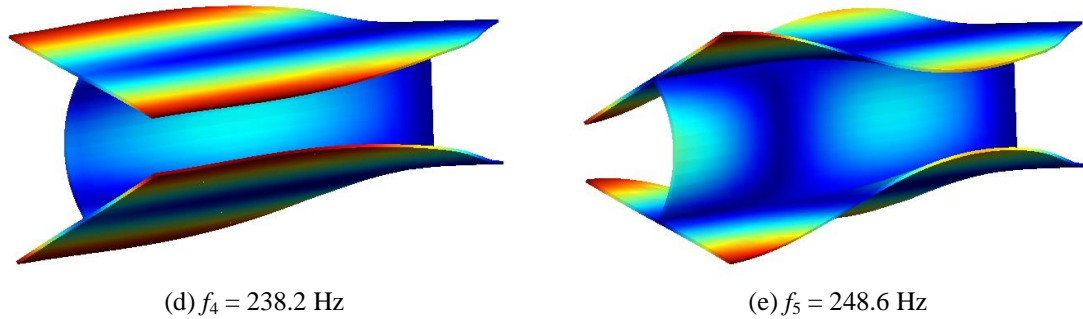


Fig. 17 Continued

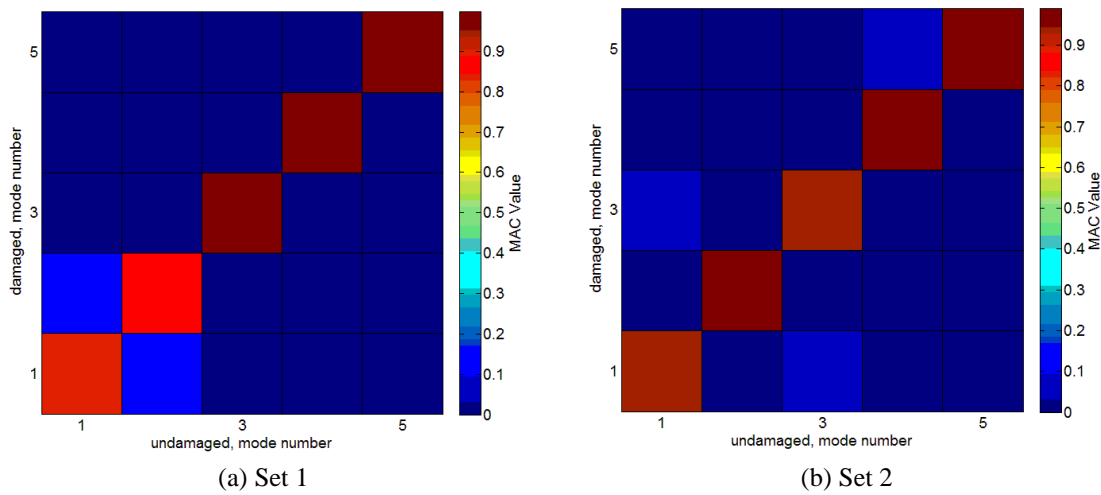


Fig. 18 MAC matrices for the I-Beam, multi-damage cross-section, 8L9

structures have either bending-torsion couplings or severe shell-like phenomena. Classical models are inadequate, and would require higher-order TE expansions ($N > 7$).

- The component-wise features of LE make this model able to deal with local and inhomogeneous damage distributions.
- The MAC matrix is slightly influenced by the local root damage.

7. Conclusions

This paper has presented free vibration analyses of damaged beams. Deep and thin-walled beams were considered. Analyses were carried out by means of classical beam models, namely the Euler-Bernoulli and Timoshenko models; refined 1D models based on Taylor-like expansions of the unknown variables; refined 1D models based on Lagrange expansions. Solid and shell models were employed for comparison purposes. The 1D models were built through the Carrera Unified Formulation (CUF). The CUF has hierarchical capabilities that allow us to deal with any order models with no need of ad hoc formulations. The 1D models based on the Lagrange expansions

(LE), in particular, have component-wise (CW) capabilities. The use of CW features leads to models that provide high-fidelity geometrical and material descriptions of the structure. No reference axes or surfaces are, in fact, needed to define an LE model. Furthermore, the use of homogenised material characteristics can be avoided.

In this paper, the damage was introduced by means of reduced stiffness areas. Globally and locally damaged beams were considered. The former were damaged along the entire span. The latter had damages in given portions of the span. Various cross-section damage distributions were considered ranging from homogenously damaged sections to locally damaged cross-sections.

The results suggest that

- As known from previous CUF works, advanced 1D models are necessary to deal with a number of non-classical effects, such as torsion, bending/torsion couplings, local effects, and cross-section distortions. The presence of damage worsens the majority of these phenomena. For instance, local effects may arise in bending modes. Therefore, the use of advanced 1D models is compulsory in the case of damaged structures.
- The effect of damage on the natural frequencies and modal shapes depends on a number of parameters. Such as the damage location, intensity and the extension. As known in the literature, it may be very difficult to detect these effects in the case of poorly damaged structures.
- It is important to notice that, for a given damage, the effects on the free vibrations depend on the modal shaped considered. Bending, torsional, or shell-like modes can be affected differently. It is important to be able to evaluate all these modes in order to improve the damage detection capabilities
- As expected, the computational cost of the advanced beam models is very low with respect to the solid model.
- Thin-walled beams require LE models to deal with torsion and shell-like modes in which severe cross-sectional deformations may occur. Such models are as accurate as shell FEs, but fewer DOFs are required.
- The presence of damage makes the use of LE necessary even for bending modes. LE are, in fact, component-wise models in which the local material and geometrical characteristics are retained, and LE can be locally refined where needed. All these features make the detection of local effects, due, for instance, to local stiffness losses, easier to deal with.
- As known from previous works of the authors, classical beam models provide acceptable accuracies for bending modes only. However, since damage can cause bending-torsion coupling, the use of classical beam models for damaged structures should be avoided.
- The effect of a damage on a natural frequency depends on the modal shape to a great extent. As soon as a damage is in place, there may be a shift in the modal shapes with respect to the undamaged configuration. For instance, shell-like modes could appear with lower frequencies than bending modes. Higher the damage, more important this effect.
- LE component-wise models are particularly powerful for the analysis of locally damaged structures and thin-walled beams. Such models provide results as accurate as those from a shell or a solid model. However, LE usually requires much fewer DOFs.

The use of CUF models for the analysis of damaged structures may have interesting outcomes as soon as damage detection is considered. Thanks to its computational efficiency and high accuracy, CUF may improve classical damage detection techniques. CUF provides, in fact, fast and reliable results for damaged structures. Furthermore, CUF could be exploited to create a database of possible damage scenarios to be used to compare to experimental data.

References

- Allemang, R.J. and Brown, D.L. (1982), "A correlation coefficient for modal vector analysis", *Proceedings of the 1st SEM International Modal Analysis Conference*, Orlando, FL, November.
- Balsamo, L. and Mukhopadhyay, S., Betti, R. and Lus, H. (2013), "Damage Detection Using Flexibility Proportional Coordinate Modal Assurance Criterion", *Topics in Modal Analysis, Volume 7: Proceedings of the 31st IMAC, A Conference on Structural Dynamics, 2013, Conference Proceedings of the Society for Experimental Mechanics Series 45*.
- Berdichevsky, V.L., Armanios, E. and Badir, A. (1992), "Theory of anisotropic thin-walled closed-cross-section beams", *Compos. Eng.*, **2**(5-7), 411-432.
- Bernoulli, D. (1751), *Commentarii Academiae Scientiarum Imperialis Petropolitanae*, Petropoli. Chapter, De vibrationibus et sono laminarum elasticarum.
- Capozuzza, R. (2014), "Vibration of CFRP cantilever beam with damage", *Compos. Struct.*, **116**, 211-222.
- Carrera, E. (2002), "Theories and finite elements for multilayered, anisotropic, composite plates and shells", *Arch. Comput. Meth. Eng.*, **9**(2), 87-140.
- Carrera, E. (2003), "Theories and finite elements for multilayered plates and shells: a unified compact formulation with numerical assessment and benchmarking", *Arch. Comput. Meth. Eng.*, **10**(3), 216-296.
- Carrera, E., Cinefra, M., Petrolo, M. and Zappino, E. (2014), *Finite Element Analysis of Structures through Unified Formulation*, John Wiley & Sons.
- Carrera, E. and Giunta, G. (2010), "Refined beam theories based on a unified formulation", *Int. J. Appl. Mech.*, **2**(1), 117-143.
- Carrera, E., Giunta, G., Nali, P. and Petrolo, M. (2010a), "Refined beam elements with arbitrary cross-section geometries", *Comput. Struct.*, **88**(5-6), 283-293.
- Carrera, E., Giunta, G. and Petrolo, M. (2011), *Beam Structures: Classical and Advanced Theories*, John Wiley & Sons.
- Carrera, E., Maiarù, M. and Petrolo, M. (2012a), "Component-wise analysis of laminated anisotropic composites", *Int. J. Solid. Struct.*, **49**(13), 1839-1851.
- Carrera, E., Pagani, A. and Petrolo, M. (2012b), "Component-wise method applied to vibration of wing structures", *J. Appl. Mech.*, **80**(4), 041012.
- Carrera, E., Pagani, A. and Petrolo, M. (2013a), "Classical, refined and component-wise analysis of reinforced-shell structures", *AIAA J.*, **51**(5), 1255-1268.
- Carrera, E. and Petrolo, M. (2012a), "Refined beam Elements with only displacement variables and plate/shell capabilities", *Meccanica*, **47**(3), 537-556.
- Carrera, E. and Petrolo, M. (2012b), "Refined one-dimensional formulations for laminated structure analysis", *AIAA J.*, **50**(1), 176-189.
- Carrera, E., Petrolo, M. and Nali, P. (2010b), "Unified formulation applied to free vibrations finite element analysis of beams with arbitrary section", *Shock Vib.*, **18**(3), 485-502.
- Carrera, E., Petrolo, M. and Zappino, E. (2012c), "Performance of CUF approach to analyze the structural behavior of slender bodies", *J. Struct. Eng.*, **138**(2), 285-297.
- Carrera, E., Zappino, E. and Petrolo, M. (2013b), "Analysis of thin-walled structures with longitudinal and transversal stiffeners", *J. Appl. Mech.*, **80**(1), 011006.
- El Fatmi, R. and Ghazouani, N. (2011), "Higher order composite beam theory built on Saint-Venant solution. Part-I: Theoretical developments", *Compos. Struct.*, **93**(2), 557-566.
- Euler, L. (1744), *De curvis elasticis*, Lausanne and Geneva, Bousquet.
- Fayyadh, M.M., Razak, H.A. and Ismail, Z. (2011) "Combined modal parameters-based index for damage identification in a beamlike structure: theoretical development and verification", *Arch. Civil Mech. Eng.*, **11**(3), 587-609.
- Gopalakrishnan, S., Ruzzene, M. and Hanagud, S. (2011), *Computational Techniques for Structural Health Monitoring*, Springer.
- Kapania, K. and Raciti, S. (1989a), "Recent advances in analysis of laminated beams and plates, Part I: shear

- effects and buckling”, *AIAA J.*, **27**(7), 923-935.
- Kapania, K. and Raciti, S. (1989b), “Recent advances in analysis of laminated beams and plates, Part II: vibrations and wave propagation”, *AIAA J.*, **27**(7), 935-946.
- Ladéveze, P., Sanchez, P. and Simmonds, J. (2004), “Beamlike (Saint-Venant) solutions for fully anisotropic elastic tubes of arbitrary closed cross-section”, *Int. J. Solid. Struct.*, **41**(7), 1925-1944.
- Mukhopadhyay, S., Lus, H., Hong, L. and Betti, R. (2012), “Propagation of mode shape errors in structural identification”, *J. Sound Vib.*, **331**, 3961-3975.
- Pérez, M.A., Gil, L., Sánchez, M. and Oller, S. (2014), “Comparative experimental analysis of the effect caused by artificial and real induced damage in composite laminates”, *Compos. Struct.*, **112**, 169-178.
- Salawu, O.S. and Williams, C. (1995), “Bridge assessment using forced-vibration testing”, *J. Struct. Eng.*, **121**(2), 161-173.
- Schardt, R. (1994), “Generalized beam theory - An adequate method for coupled stability problems”, *Thin Wall. Struct.*, **19**(2-4), 161-180.
- Timoshenko, S.P. (1921), “On the corrections for shear of the differential equation for transverse vibrations of prismatic bars”, *Philos. Mag.*, **41**, 744-746.
- Wang, Y., Liang, M. and Xiang, J. (2014), “Damage detection method for wind turbine blades based on dynamics analysis and mode shape difference curvature information”, *Mech. Syst. Signal Pr.*, **48**, 351-367.
- Zhang, Z., Shankar, K., Morozov, E.V. and Tahtali. M. (2014), “Vibration-based delamination detection in composite beams through frequency changes”, *J. Vib. Control*, DOI: 10.1177/1077546314533584.
- Zhao, J. and Zhang, L. (2012), “Structural damage identification based on the modal data change”, *Int. J. Eng. Manuf.*, **4**, 59-66.